THE JOURNAL OF PHYSICAL CHEMISTRY C

Article

Cite This: J. Phys. Chem. C 2018, 122, 14289−14295

pubs.acs.org/JPCC

Thermal Explosions of Polymer-Bonded Explosives with High Time and Space Resolution

Zhiwei Men,[†,‡] Kenneth S. Suslick,[†] and Dana D. Dlott[†,*]

[†]School of Chemical Sciences, University of Illinois at Urbana−Champaign, 600 S. Mathews Avenue, Urbana, Illinois 61801, United States

[‡]College of Physics, Jilin University, Qianjin Street # 2699, Changchun, Jilin Province 130012, P. R. China

Supporting Information

ABSTRACT: It has always been difficult to observe thermally induced explosions, because the onset is unpredictable. By use of ultrasound to induce intense, localized frictional heating at the surface of crystals embedded in a flexible polymer, we have created a new method for the initiation of microexplosions under conditions where temporal and spatially resolved observations can be made. Specifically, we report the use of ultrasound to flash-heat polymer-embedded <500 μm RDX $(CH_2NNO_2)_3$ and HMX $(CH_2NNO_2)_4$ crystals at rates >10 000 K/s. By using this extremely rapid heating on small samples, we were able to confine the explosion to narrow regions in time and space. The explosion was measured using dual thermal imagers providing temporal and spatial resolutions of 1 μs and 15 μm. Surprisingly, the explosions always occurred in *two stages*, an initial 0.1 ms stage and a subsequent 100 ms stage. The first stage of RDX explosion (2500 K lasting 140 μs) was less violent than that for HMX (4400 K lasting 70 μs), which is consistent with the general observation that HMX is regarded as a higher-performance explosive. The origin of the two-stage explosion originates from how the explosive chemistry is modulated by the mechanical behavior of the flexible polymer at the interface with the explosive crystal. The crystal explosion created a blast that produced a cavity in the surrounding polymer filled with reactive gases; subsequent ignition of the gases in that cavity caused the second-stage explosion.

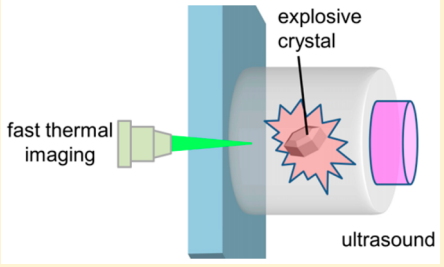

1. INTRODUCTION

It has been difficult to observe the early stages of explosions with high time and space resolution, especially thermally induced explosions.[1] Unlike detonations, which can be forcibly triggered and synchronized by an incoming shock wave, thermal explosions induced by heating of explosive charges appear unpredictably in time and in space. By use of ultrasound to induce intense, localized frictional heating at the surface of crystals embedded in a flexible polymer, we have created a new method for the initiation of microexplosions under conditions where temporal and spatially resolved observations overcome the past synchronization and spatial limitations; combined with thermal imaging detectors with long record lengths, we are able to routinely capture thermally induced explosive events. Specifically, we localized the thermal explosion in space by heating individual small (<500 μm) explosive crystals, either RDX $(CH_2NNO_2)_3$ or HMX $(CH_2NNO_2)_4$, encased in a flexible polymer binder, Sylgard 182, a *poly*-dimethylsiloxane (PDMS).

Thermal explosions of macroscopic size have previously been successfully synchronized only by use of a laser trigger approach by Smilowitz and co-workers,[1,2] who gradually preheated a 1/2" diameter explosive cylinder into the thermal runaway regime and then triggered the explosion with a 150 μs laser pulse. These laser-triggered explosions were probed with embedded thermocouples[2] and proton and X-ray radiography.[3−6]

In 2014, our group described an ultrasound flash-heating technique to frictionally heat polymer-bonded explosives at rates of more than 10^4 K/s per second (e.g., to 1000 K in 100 ms).[7,8] The flash-heated explosives were monitored by thermal imaging microscopy. In initial trials, driving solid inclusions embedded in a polymer with ultrasound did not produce high-speed heating. We discovered that the heating rate could be dramatically increased if the polymer were de-adhered from the solid by applying a small amount of powdered or liquid lubricant to the solid's surface,[7,8] as depicted in Figure 1. Instead of the solid inclusion oscillating synchronously with the polymer, the lubricant, by breaking the polymer−solid adhesion, allowed the crystal surfaces and polymer to rub against each other at 20 kHz, causing rapid frictional heating.[7]

Roberts and co-workers subsequently showed that a similar rapid ultrasonic heating effect could be produced by mechanically debonding crystals from surrounding polymer[9] and concluded that friction between the crystal and the moving binder at the crystal surface produced rapid frictional heating leading to an explosion.[9] The sensitivity of explosives to rubbing is well-known, and friction sensitivity has been studied for many explosives.[10] But unlike the usual friction initiation measurements that use a belt sander,[11] a piece of sandpaper on

Received: March 13, 2018
Revised: June 7, 2018
Published: June 7, 2018

DOI: 10.1021/acs.jpcc.8b02422
J. Phys. Chem. C 2018, 122, 14289−14295

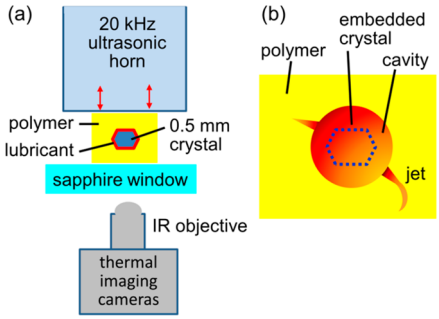

Figure 1. (a) Polymer-encased crystal of RDX or HMX was pressed between a 20 kHz ultrasonic horn and a sapphire window. (b) When the crystal exploded, the blast created a cavity in the surrounding polymer. Two-stage explosions were observed with dual thermal imaging cameras, together having high time and space resolution.

the striker of a drop hammer,[12] or a moving pendulum,[10] with ultrasound, the 20 kHz rubbing is extremely rapid, and multiple surfaces of the crystal may rub against the surrounding polymer.[7,9]

RDX and HMX are closely related high-performance insensitive high explosives that have been studied extensively in thermal explosion[13,14] (heat-initiated) and detonation[15] (shock-initiated) modes. They are usually used in the form of polymer-bonded explosives (PBX). As a model of such PBX, we have studied 0.5 mm RDX and HMX crystals embedded in a block of PDMS. These polymer-explosive composites were frictionally heated with ultrasound at such a high rate (>10^4 K/s) that we could measure the time and space evolution of the ensuing thermal explosions with thermal imaging. We obtained unprecedented 1 μs time resolution and 15 μm spatial resolution of the thermal explosions. An unexpected finding was the role of polymer confinement, which caused the RDX and HMX thermal explosions to occur in two stages, an initial 0.1 ms explosion and a subsequent 100 ms explosion.

In earlier experiments, rapid heating of explosive crystals was monitored by a mid-infrared (mid-IR: 3.7−4.8 μm) video camera having a frame rate of 120 Hz (8.3 ms interframe interval) viewing through an IR microscope giving near-diffraction-limited spatial resolution of 15−20 μm.[7,8] Unfortunately, the 8.3 ms interframe interval of the video camera was too slow to time resolve thermal explosions. Even though the response time of its HgCdTe (MCT) detector elements was 1 μs, the frame rate was limited by time needed to read out the 640 × 512 images (327 680 pixels) with a 4 MHz analog-to-digital (A/D) converter. Recognizing this limitation, we obtained an additional mid-IR detector of a new type that sacrifices image resolution in favor of high readout speed. It consisted of a linear array of 32 MCT detector elements with 112 μm spacing (3.58 mm image length). For the linear array, the readout is fast, because each detector channel has its own 4 MHz A/D converter. Obtaining four data points each microsecond allows us to realize the full bandwidth of the MCT detector elements. The linear array produces 4 000 000 images per second, giving the temperature, via single-color pyrometry, at 32 points along a line running through the explosion, and it does so 33 000 times faster than the video camera. The linear array A/D converters have a 520 K memory record, which limits each single-shot record to a time interval of 13.1072 ms, so we have to have the ability to synchronize the explosion within that finite time window. The complementary video camera and linear array thermal imagers produced a combination of higher-resolution images with relatively poor time resolution and lower-resolution images with far higher time resolution.

2. EXPERIMENTAL METHODS

2.1. Sample Fabrication. RDX or HMX powders were dissolved in acetone and recrystallized once to ensure purity. The ∼0.5 mm RDX or HMX crystals were grown by slow evaporation from acetone. Each sample for thermally induced explosions consisted of a polymer-encased crystal with a thin lubricant coating[7,8] on an IR-transmitting sapphire window, as depicted in Figure 1.

The lubricant was M_w 400 poly ethylene glycol (PEG) from Sigma-Aldrich. The crystals were dipped into the PEG and air-dried on a glass slide for 15 min. The coated crystals were baked at 120 °C for 15 min, and then, the procedure was repeated to achieve a homogeneous PEG coating a few μm thick. In sample preparation, the polymer lubricant and polymer binder were cured by heating at 100 °C for 15 min. Calorimetry and gravimetric analysis have shown no significant thermal decomposition for RDX or HMX for brief exposures to temperatures below 200 °C.[16]

The polymer binder was Sylgard 182 from Dow Corning. Sylgard is a trade name for a poly dimethylsiloxane (PDMS) rubber. We used a 10:1 ratio (resin/hardener) by weight and degassed the mixture under vacuum before curing. A 300 μm layer of PDMS was spread onto a 25.4 mm sapphire window and cured. Both sapphire and PDMS have adequate transparency in the mid-IR region detected by our thermal imagers. A second 500 μm PDMS layer was added, and while this second layer was semiliquid, the PEG-coated crystals were submerged in PDMS with tweezers. After the PDMS−crystal layer was cured, a third 500 μm thick PDMS capping layer was spread over the crystal and cured to fully encase the crystal.

2.2. Ultrasound Heating. The ultrasonic heating apparatus was described previously.[7,8,17] As depicted in Figure 1a, a 13 mm diameter 20 kHz Ti acoustic horn (CV-33, Sonics and Materials Inc.) was pressed against the PDMS capping layer using a spring-loaded holder (not shown) to frictionally heat the polymer-confined crystals. We varied the springs to get good acoustic contact without deforming the crystals and got good results with a spring force of 10^6 N/m^2.[7] The amplitude of the 20 kHz horn was adjusted by a controller (Vibracell VCX-750, Sonics and Materials, Inc.) in the range between 20 and 100% of the peak amplitude of 114 μm[7] to produce prompt thermal explosions with minimal jitter in time-to-explosion.

2.3. High-Speed Thermal Imaging. A delay generator was used to trigger the ultrasonic horn and the IR detectors.[7] The horn was pulsed for 1 s at a start time denoted t = 0. The video camera (IRE-640M, Sofradir-EC Inc.) had 15 μm pitch 640 × 512 MCT detector elements cooled to 90 K and a cooled prefilter that transmitted light only in the mid-IR 3.7−4.8 μm range. Camera characterization and temperature calibration against a blackbody standard were discussed previously,[7] where we measured the temperature dependence of RDX emissivity. Because of the close similarity in chemical structure of RDX and HMX, here we assumed the RDX emissivity for HMX. The camera viewed the sample through the sapphire window and thin PDMS bottom layer using a 1× mid-IR microscope objective with N.A. = 0.22 (Asio 1X, Janos Tech, Keene, NH). The working distance from objective to crystal was 60 mm. The linear array detector (TEDAS-3200,

DOI: 10.1021/acs.jpcc.8b02422
J. Phys. Chem. C 2018, 122, 14289−14295

Infrared Systems Development Corp.,Winter Park, FL) was liquid N_2 cooled. It used an identical mid-IR microscope objective. Its 0.1 mm 32 MCT detector elements with 0.112 mm pitch and cooled optical prefilter were designed to closely match the spectral response of the video camera, so the calibration procedure was the same as used with the video camera.

3. RESULTS

We did a number of runs with different 0.5 mm RDX and HMX crystals. Each run differed in details such as time-to-explosion due to variations in crystal size and shape and crystal−polymer adhesion but were overall quite similar.

The video images in Figures 2 and 3 were selected frames extracted from movies taken by the video infrared camera.

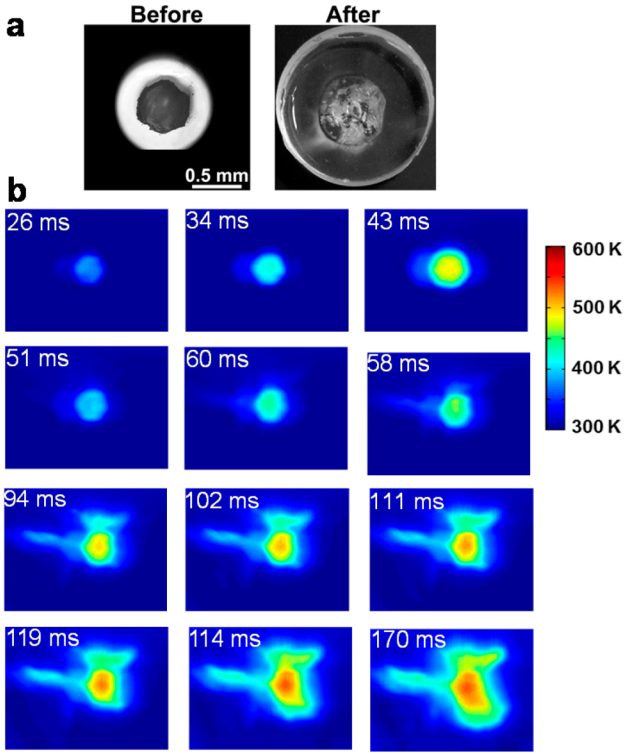

Figure 2. Two-stage explosion was observed in the infrared imaging of a polymer-encased RDX crystal frictionally heated with a 1 s pulse of ultrasound energized at $t = 0$. The two stages of the explosion are shown explicitly in the thermal images, with the first maximum in heating occurring at 43 ms and the second, larger thermal maximum at 114 ms. (a) Optical micrographs of the crystal before and after explosion; note that the fields of view are different, while the magnification has been kept constant for comparison. (b) Thermal images from 26 to 170 ms after initiation of ultrasonic heating. For both (a) and (b), the scale bar is the same for all image panels.

Representative movies are available as Supporting Information. Figure 2 shows a polymer-confined RDX crystal explosion, and Figure 3 shows a polymer-confined HMX crystal explosion. The polymer was PDMS. Visible light images of the approximately 0.5 mm crystals before and after ultrasound are shown at the top of the figures. The "after" pictures clearly show that powerful explosions had taken place. With RDX in Figure 2, in the image at 43 ms, a 470 K hot spot appeared that was about the size of the crystal. We attribute this hot spot to a ball of hot dense gas in a roughly spherical polymer cavity

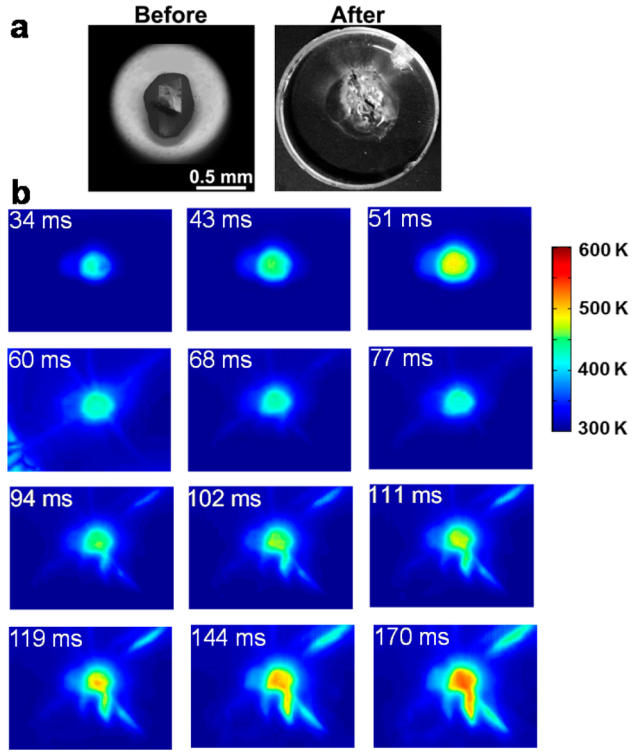

Figure 3. Two-stage explosion was observed in the infrared imaging of a polymer-encased HMX crystal frictionally heated with a 1 s pulse of ultrasound energized at $t = 0$. The two stages of the explosion are shown explicitly in the thermal images, with the first maximum in heating occurring at 51 ms and the second, larger thermal maximum at 170 ms. (a) Optical micrographs of the crystal before and after explosion; note that the fields of view are different, while the magnification has been kept constant for comparison. (b) Thermal images from 34 to 170 ms after initiation of ultrasonic heating. For both (a) and (b), the scale bar is the same for all image panels.

produced by the initial RDX explosion. A second explosion was observed in the images beginning at 94 ms. The second explosion lasted much longer, at least 70 ms, and it appeared slightly hotter, about 550 K. During the second explosion, jets of hot gas pierced the polymer confinement. Significantly, in all video imaging of these events, we always observed two-stage explosions.

With HMX (Figure 3), the explosion was similar to that of RDX and again showed two distinct stages. The first HMX explosion started at 56 ms vs 43 ms for RDX, but among multiple runs, there was enough variation in time-to-explosion that we cannot say that RDX and HMX have intrinsically different times-to-explosion. We believe that the variation in the initial explosion time probably reflects slight differences in crystal size, shape, and mechanical contacts (i.e., adhesion) to the surrounding polymer.

3.1. Fast Linear Array Images. The video camera was adequate for the slower second explosions but incapable of time resolving the first explosions. We used the much faster linear mid-IR detector array to focus on the first explosions, as shown in Figures 4−6. Figures 4 and 5 are linear array outputs showing the RDX and HMX first explosions in detail. Note the linear array data were obtained from different but similar-size RDX and HMX crystals from the ones used in the video imaging in Figures 2 and 3. We indicated the approximate RDX and HMX crystal positions in Figures 4b and 5b based on

DOI: 10.1021/acs.jpcc.8b02422
J. Phys. Chem. C 2018, 122, 14289−14295

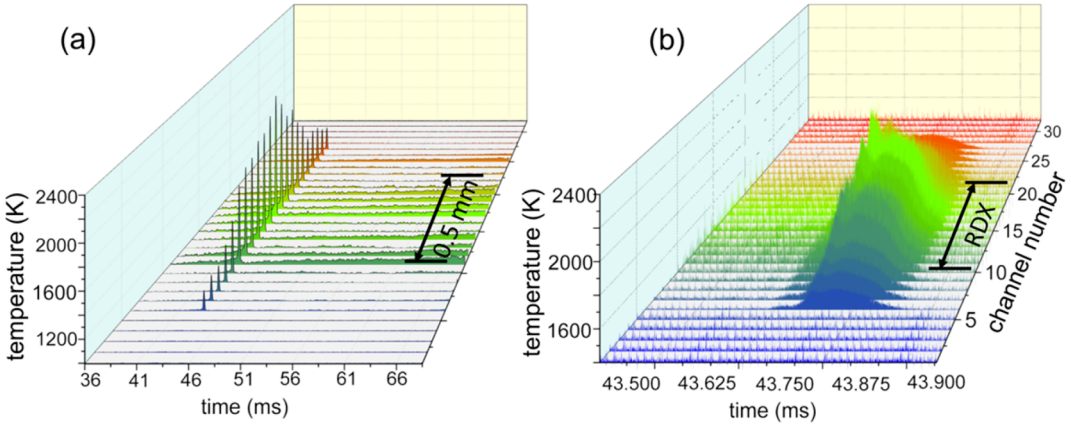

Figure 4. (a) Thermal image from a linear array of the first-stage explosion of a polymer-encased RDX crystal. (b) Expanded time scale. The spacing between each of the 32 channels of the linear array was 0.112 mm. The block labeled RDX indicates the approximate position of the RDX crystal prior to ultrasound flash heating.

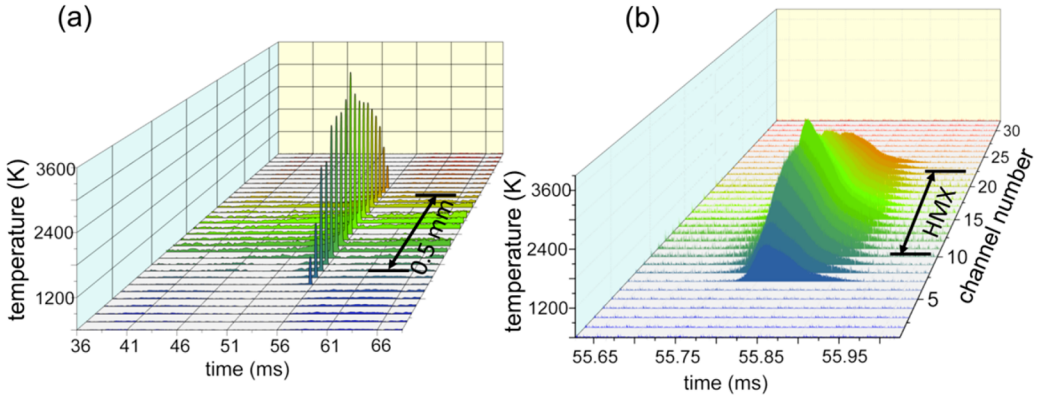

Figure 5. (a) Thermal image from a linear array of the first-stage explosion of a polymer-encased HMX crystal. (b) Expanded time scale. The spacing between each of the 32 channels of the linear array was 0.112 mm. The block labeled HMX indicates the approximate position of the HMX crystal prior to ultrasound flash heating.

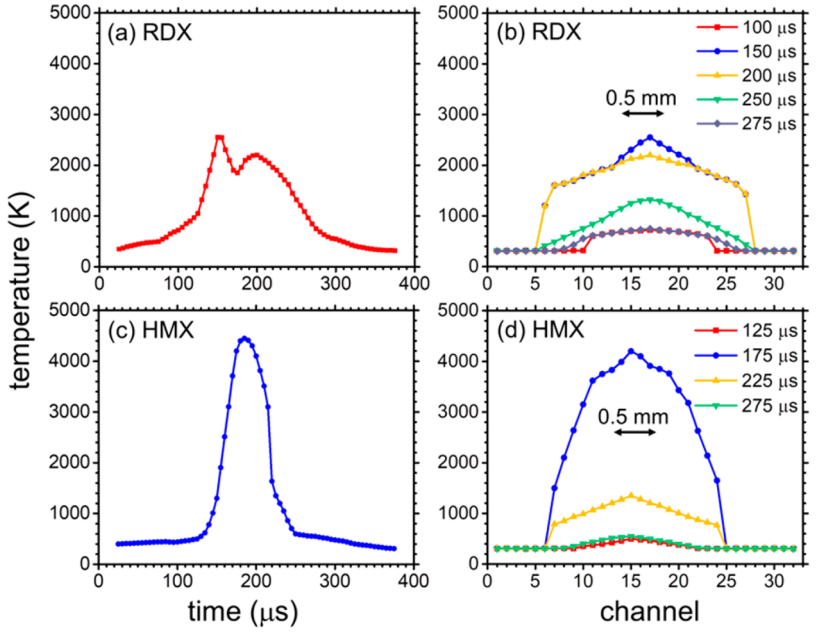

Figure 6. (a,c) Time-dependent temperatures from the first thermal explosion taken from a strip 0.3 mm wide running through the center of the 0.5 mm RDX and HMX crystals. Time zero is arbitrary. (b,d) Spatial variation of temperatures from RDX and HMX thermal explosions at various locations. The spacing between channels of the linear array was 0.112 mm.

DOI: 10.1021/acs.jpcc.8b02422
J. Phys. Chem. C 2018, 122, 14289−14295

visible microscope images taken before ultrasound heating. The spacing between the individual channels of the linear array was 0.112 mm. Figures 4a and 5a show the full 32 ms linear array record. In those images, the explosion appeared instantaneously at 43 ms for RDX and 56 ms for HMX.

The first-stage explosions can be seen in more detail in Figures 4b and 5b, which are the same data as in Figures 4a and 5a but on an expanded time scale. The first explosions were hotter and faster than they appeared in the video images, because the video camera's 8 ms interframe rate did not allow us to fully resolve the durations and peak temperatures.

We analyzed the linear array images by plotting in Figure 6 the temperatures along strips three channels wide running through the middle of the 0.5 mm crystals along the time and position directions. The strips were 0.336 mm wide, and the time- and position-dependent temperatures were linear averages across the strips.

Time-dependent temperatures for RDX and HMX are shown in Figure 6a,c. The displayed data points every 5 μs were linear averages of the 20-point detector output within each time interval. Time zero in Figure 6a,c was set arbitrarily so that the explosion peak temperatures appeared near the center of the plots. The peak temperatures and explosion durations (full-width half maxima in Figure 6a,c) were 2500 K and 140 μs for RDX and 4400 K and 70 μs for HMX. The HMX thermal explosion was significantly more violent, faster, and hotter than the thermal explosion of RDX. RDX appears to have a double-peaked temperature profile, which most likely is due to the way the spatial profile of temperature changes with time. Although the adiabatic flame temperatures of RDX and HMX are similar,[18] this is a transient measurement, and the HMX temperature is likely higher due to its faster rate of energy release. From the video images in Figures 2 and 3, we can estimate the approximate rate the explosive crystals were heated by ultrasound. In the run-up to explosion, we see RDX at ~450 K at 34 ms (Figure 2) and HMX at ~500 K in 43 ms (Figure 3). So the ultrasound heating rate was 12×10^4 K/s. From Figure 6a,c, we can estimate the approximate heating rates due to the thermal explosion. The rise times of the thermal explosions were roughly 50 μs, and the temperatures were 2500 K for RDX and 4400 K for HMX, giving heating rates of 5 or 9×10^7 K/s.

Position-dependent temperature profiles are shown in Figure 6b,d. These profiles indicate that hot gases (the blast) expanded outward significantly from their origin during the first-stage explosions. On the basis of the nominally spherical distribution of the high temperatures in Figures 1 and 2 during the first-stage explosions, the initial blast appears to be confined within a roughly spherical polymer cavity surrounding the exploding crystal, as depicted in Figure 1b. At the earliest times, when the explosion became hot enough to see with the thermal imager, ~100 μs, the hot material from the 0.5 mm crystal appears to be confined within a cavity about 1.5 mm in diameter. At the peak of the explosion, this cavity has expanded to about 2.5 mm diameter for RDX and 2.2 mm for HMX. Thus, the maximum cavity diameter was roughly 4−5 times the size of the originating crystal. With the assumption of a roughly spherical cavity with volume proportional to the cube of the diameter, the blast has expanded to a volume roughly 50−100 times the original crystal volume. We can crudely estimate the expansion velocity from Figure 6b, where the blast has moved about 5 mm in about 100 μs. This estimated velocity is 50 m/s, and it is subsonic (Mach 1 in air is 331 and 1120 m/s in PDMS).

As seen in Figure 6b,d, the high temperatures during the first-stage explosions, after some expansion, stopped abruptly at what was presumably the inner wall of the polymer cavity. Since the expansion velocity was subsonic, the steepness of the temperature rise at the inner wall of the polymer cavity does not support the idea of a blast wave propagating outward from the crystal. A blast wave consists of hot gas expanding supersonically from an explosive core, and it should have a sharp leading shock front of compressed gas. Instead, the steep temperature rise appears to be due to hot gas pileup at the inner surface of the cavity, caused by the resistance of the stretched polymer to further expansion. Figure 6b,d also provide some evidence in the longer-time temperature distributions (e.g., after 275 μs) that the polymer cavity partially collapsed after the peak temperature was reached. Our imaging results show that the polymer surrounding the exploding crystal first underwent a roughly spherical expansion followed by a partial collapse and a second explosion that pierced the cavity in a few locations, creating escaping jets of hot gases. In this regard, we characterize the behavior of the polymer as "partially confining".

4. DISCUSSION

Using ultrasound, we frictionally flash-heated polymer-embedded RDX and HMX crystals at rates $>10^4$ K/s, causing sudden-onset thermal explosions. With our dual complementary thermal imaging detectors, we could observe the temperature distributions of the two stages of the thermal explosions in time and space. In general terms, the HMX explosion was more violent than the RDX explosion, consistent with the general observation that HMX is regarded as a higher-performance explosive.[10]

It is no surprise that a confining medium such as a polymer binder can strongly affect the chemistry of a small exploding solid, even if the polymer does not interact chemically with the explosive. After all, an unconfined heated RDX or HMX crystal will combust without explosion,[19] whereas a confined heated RDX or HMX crystal, as we see here, will explode. Since we have no evidence for energetic reactions between the explosive and the surrounding PDMS, which is notably chemically inert, the effects of the confining polymer appear to originate primarily from the way the polymer affects the mechanics of the explosion.

The ability of a partially confining elastic medium to produce a two-stage explosion was unexpected but not difficult to understand. We believe that the first explosion is a solid-state explosion and that the second explosion is a gas-phase explosion. Initially, within the tight polymer confinement, the rapidly heated RDX and HMX crystals begin to explode and expel a blast of hot gases with enough force to create a gas-filled cavity in the PDMS, as depicted in Figure 1b. Since the PDMS provided only partial confinement, the explosive reaction did not proceed to completion during the first stage of explosion. The slower-reacted chemical species in this complex chemical stew[20−22] were quenched by the adiabatic cooling and reduced molecular collision rates in the expanding blast, and they must contain enough energy to power the second-stage explosion. The second stage, then, is a kind of afterburn of the unreacted gases in the blast. Since the blast is contained within the polymer cavity, this afterburn reaction is a confined explosion, at least until the confinement was lifted

DOI: 10.1021/acs.jpcc.8b02422
J. Phys. Chem. C 2018, 122, 14289−14295

when the hot gas jetted out of the cavity (schematic in Figure 1b and images in Figures 2 and 3). We cannot be sure of the mechanism that triggered the second explosions. It might be adiabatic heating from the compression of the rebounding polymer cavity or it might be determined by gas-phase chemical kinetics.

Although it might seem that the two-stage explosion is a special case limited to the particular system studied here, two-stage explosions were also observed under vastly different circumstances. Previously, we studied HMX explosions initiated by short-duration (~5 ns) shock waves produced by flyer plate impacts at km/s velocities.[23,24] We measured time-dependent temperature profiles of the exploding HMX using nanosecond time-resolved optical pyrometry.[23−25] The first part of the explosion, in high-density shock-compressed HMX, occurred at 7000 K. The shock-compressed HMX then underwent a nanosecond expansion as the shock unloaded, causing the temperature to drop to ~3000 K. Abruptly, there was a second, 4000 K explosion. This second explosion was again an afterburn of energetic species that did not have time to react prior to the expansion.[23−25] So it is possible that two-stage explosions might occur in a wide variety of energetic material formulations, whenever an exploding grain is partially confined by its surroundings, allowing for both solid-state and secondary gas-phase explosions. Two-stage explosions of this type would be difficult to observe in large explosive charges, although they may nevertheless be there.

5. SUMMARY AND CONCLUSION

We have resolved thermally induced explosions in space and time using ultrasound to frictionally heat an explosive-polymer composite along with two complementary kinds of thermal imagers. The HMX explosion was more violent than the RDX explosion, consistent with the general observation that HMX is regarded as a higher-performance explosive.[10] The PDMS polymer encasing the charge provided partial confinement due to its flexibility: with partial confinement, there were two stages of explosion, a faster process with heating rates as high as tens of millions of K/s at near-condensed-phase densities and a later slower process in the polymer bubble produced from the blast from the exploding crystals. The observation of two-part explosions with both shock initiation and flash heating suggests that more attention should be paid to understanding the role of mechanical processes in the surrounding medium in influencing the chemical kinetics of explosions.

With partial confinement, these crystals exploded in two stages, a faster stage occurring at condensed-phase densities and a slower stage in the confined gases produced by the exploding crystals. The observation of two-part explosions with both shock initiation and flash heating indicates that more attention should be paid to the effects of mechanical processes in the medium surrounding the explosive on the chemical kinetics.

The creation of this new technique to temporally and spatially resolve thermally induced explosions opens a variety of avenues for future exploration. For examples, the effects of scale of size of the explosive crystals (both smaller and larger) and the impact of the mechanical properties of the polymer (e.g., changes in elasticity of the polymer from the degree of cross-linking) on the confinement process and the two-stage explosion process both remain open questions.

■ ASSOCIATED CONTENT

Supporting Information

The Supporting Information is available free of charge on the ACS Publications website at DOI: 10.1021/acs.jpcc.8b02422.

Thermal imaging of HMX thermal explosion (WMV)

Thermal imaging of RDX thermal explosion (WMV)

■ AUTHOR INFORMATION

Corresponding Author

*E-mail: dlott@illinois.edu (D.D.D.)

ORCID

Kenneth S. Suslick: 0000-0001-5422-0701

Dana D. Dlott: 0000-0001-8719-7093

Notes

The authors declare no competing financial interest.

■ ACKNOWLEDGMENTS

The research described in this study was based on work supported by the US Air Force Office of Scientific Research under FA9550-16-1-0042. Zhiwei Men acknowledges support from the Office of China Postdoctoral Council for work performed at the University of Illinois.

■ REFERENCES

(1) Smilowitz, L.; Henson, B. F.; Sandstrom, M. M.; Romero, J. J.; Asay, B. W. Laser Synchronization of a Thermal Explosion. *Appl. Phys. Lett.* **2007**, *90*, 244102.

(2) Smilowitz, L.; Henson, B. F.; Sandstrom, M. M.; Asay, B. W.; Oschwald, D. M.; Romero, J. J.; Novak, A. M. Fast Internal Temperature Measurements in PBX9501 Thermal Explosions. *AIP Confer. Proc.* **2006**, *845*, 1211−1214.

(3) Smilowitz, L.; Henson, B. F.; Romero, J. J.; Asay, B. W.; Schwartz, C. L.; Saunders, A.; Merrill, F. E.; Morris, C. L.; Kwiatkowski, K.; Hogan, G.; et al. Direct Observation of the Phenomenology of a Solid Thermal Explosion Using Time-Resolved Proton Radiography. *Phys. Rev. Lett.* **2008**, *100*, 228301.

(4) Smilowitz, L.; Henson, B. F.; Romero, J. J.; Asay, B. W.; Saunders, A.; Merrill, F. E.; Morris, C. L.; Kwiatkowski, K.; Grim, G.; Mariam, F.; et al. The Evolution of Solid Density within a Thermal Explosion. I. Proton Radiography of Pre-Ignition Expansion, Material Motion, and Chemical Decomposition. *J. Appl. Phys.* **2012**, *111*, 103515.

(5) Smilowitz, L.; Henson, B. F.; Romero, J. J.; Asay, B. W.; Saunders, A.; Merrill, F. E.; Morris, C. L.; Kwiatkowski, K.; Grim, G.; Mariam, F.; et al. The Evolution of Solid Density within a Thermal Explosion II. Dynamic Proton Radiography of Cracking and Solid Consumption by Burning. *J. Appl. Phys.* **2012**, *111*, 103516.

(6) Smilowitz, L.; Henson, B. F.; Romero, J. J.; Oschwald, D. Thermal Decomposition of Energetic Materials Viewed Via Dynamic X-Ray Radiography. *Appl. Phys. Lett.* **2014**, *104*, 024107.

(7) Chen, M.-W.; You, S.; Suslick, K. S.; Dlott, D. D. Hot Spots in Energetic Materials Generated by Infrared and Ultrasound, Detected by Thermal Imaging Microscopy. *Rev. Sci. Instrum.* **2014**, *85*, 023705.

(8) You, S.; Chen, M.-W.; Dlott, D. D.; Suslick, K. S. Ultrasonic Hammer Produces Hot Spots in Solids. *Nat. Commun.* **2015**, *6*, 6581.

(9) Roberts, Z. A.; Casey, A. D.; Gunduz, I. E.; Rhoads, J. F.; Son, S. F. The Effects of Crystal Proximity and Crystal-Binder Adhesion on the Thermal Responses of Ultrasonically-Excited Composite Energetic Materials. *J. Appl. Phys.* **2017**, *122*, 244901.

(10) Köhler, J.; Meyer, R. *Explosives*, 4th ed.; VCH Publishers: New York, 1993.

(11) Bowden, F. P.; Yoffe, A. D. *Fast Reactions in Solids*; Butterworth Scientific: New York, 1958.

DOI: 10.1021/acs.jpcc.8b02422
J. Phys. Chem. C 2018, 122, 14289−14295

(12) Simpson, L. R.; Foltz, M. F. *LLNL Small-Scale Drop-Hammer Impact Sensitivity Test*; UCRL-ID--119665; Lawrence Livermore National Laboratory, 1995.
(13) Henson, B. F.; Smilowitz, L. B. The Chemical Kinetics of Solid Thermal Explosions. In *Non-Shock Initiation of Explosives*; Asay, B. W., Ed.; Shock Wave Science and Technology Reference Library; Springer-Verlag: Berlin, 2010; Vol. *5*.
(14) Kassoy, D. R.; Kapila, A. K.; Stewart, D. S. A Unified Formulation for Diffusive and Nondiffusive Thermal Explosion Theory,. *Combust. Sci. Technol.* **1989**, *63*, 33−43.
(15) Fickett, W.; Davis, W. C. *Detonation*; University of California Press: Berkeley, CA, USA, 1979.
(16) Lee, J.-S.; Hsu, C.-K.; Chang, C.-L. A Study on the Thermal Decomposition Behaviors of PETN, RDX, HNS and HMX,. *Thermochim. Acta* **2002**, *392*−*393*, 173−176.
(17) Chen, M.-W.; You, S.; Suslick, K. S.; Dlott, D. D. Hot Spot Generation in Energetic Materials Created by Long-Wavelength Infrared Radiation. *Appl. Phys. Lett.* **2014**, *104*, 061907.
(18) Collins, E. S.; Gottfried, J. L. Laser-Induced Deflagration for the Characterization of Energetic Materials. *Propellants, Explos., Pyrotech.* **2017**, *42*, 592−602.
(19) Oyumi, Y.; Brill, T. B. Thermal Decomposition of Energetic Materials 3. A High-Rate, in Situ, FTIR Study of the Thermolysis of RDX and HMX with Pressure and Heating Rate as Variables. *Combust. Flame* **1985**, *62*, 213−224.
(20) Chakraborty, D.; Muller, R. P.; Dasgupta, S.; Goddard, W. A., III The Mechanism for Unimolecular Decomposition of RDX (1,3,5,-Trinitro-1,3,5-Triazine), an *Ab Initio* Study. *J. Phys. Chem. A* **2000**, *104*, 2261−2272.
(21) Chakraborty, D.; Muller, R. P.; Dasgupta, S.; Goddard, W. A., III Mechanism for Unimolecular Decomposition of HMX (1,3,5,7-Tetranitro-1,3,5,7-Tetrazocine), an Ab Initio Study. *J. Phys. Chem. A* **2001**, *105*, 1302−1314.
(22) Strachan, A.; Kober, E. M.; van Duin, A. C. T.; Oxgaard, J.; Goddard, W. A. Thermal Decomposition of RDX from Reactive Molecular Dynamics. *J. Chem. Phys.* **2005**, *122*, 054502.
(23) Bassett, W. P.; Dlott, D. D. High Dynamic Range Emission Measurements of Shocked Energetic Materials: Octahydro-1,3,5,7-Tetranitro-1,3,5,7-Tetrazocine (HMX). *J. Appl. Phys.* **2016**, *119*, 225103.
(24) Bassett, W. P.; Dlott, D. D. Shock Initiation of Explosives: Temperature Spikes and Growth Spurts. *Appl. Phys. Lett.* **2016**, *109*, 091903.
(25) Bassett, W. P.; Dlott, D. D. Multichannel Emission Spectrometer for High Dynamic Range Optical Pyrometry of Shock-Driven Materials. *Rev. Sci. Instrum.* **2016**, *87*, 103107.

DOI: 10.1021/acs.jpcc.8b02422
J. Phys. Chem. C 2018, 122, 14289−14295